Journal of Molecular Catalysis B: Enzymatic 74 (2012) 209–218

Contents lists available at SciVerse ScienceDirect

Journal of Molecular Catalysis B: Enzymatic

journal homepage: www.elsevier.com/locate/molcatb

Modelling enzymatic oxidation of D-glucose with pyranose 2-oxidase in the presence of catalase

Gheorghe Maria*, Manuela Diana Ene, Iuliana Jipa

University Politehnica of Bucharest, Department of Chemical & Biochemical Engineering, Polizu Str. 1, 011061 Bucharest, P.O. 35-107, Romania

ARTICLE INFO

Article history:
Received 26 June 2011
Received in revised form
15 September 2011
Accepted 12 October 2011
Available online 19 October 2011

Keywords:
D-Glucose oxidation
Pyranose oxidase
Kinetic model
Catalase

ABSTRACT

To evaluate the activity of a commercial pyranose 2-oxidase (P_2O_x) used to catalyze the oxidation of β-D-glucose in the presence of catalase, systematically batch experiments have been carried out at 30 °C and an optimal pH = 6.5. A complex kinetic model was proposed including the main reaction (of Ping-Pong–Bi-Bi type) but also P_2O_x inactivation by the hydrogen peroxide produced, and in situ H_2O_2 decomposition by catalase (of a generalized Yano-Koya kinetics). While the presence of catalase drastically slows down the P_2O_x inactivation, a considerable decrease of the main reaction rate is observed. The estimated free enzyme rate constants match with the values reported in the literature, while turnover numbers are correlated with the catalase concentration. The model is recommended for further process developments and reactor optimization, its parameters being easily adaptable for every type of P_2O_x.

1. Introduction

Recent improvements in the synthetic biotechnology and production of modified enzymes, exhibiting desired functions, allowed a considerable progress in industrial enzyme technologies. Enzymatic reactions, displaying a high selectivity and specificity, are attractive bioengineering routes to obtain a wide range of industrial products, or present challenging applications in medical-tests, biosensor production, or emerging bio-renewable energy industries [1]. Isolated and immobilized enzymes have been used in large-scale industrial reactors, competing in terms of efficiency with the classical chemical synthesis pathways. Biocatalytic processes produce less by-products, consume less energy, and generate less environmental pollution, with using smaller catalyst concentrations and much moderate reaction conditions [2]. While intensive efforts are invested in protein engineering (recombinant enzymes), fabrication of bioactive nanostructures leads to improve the enzyme stability and its catalytic efficiency [1]. Such efforts are trying to overcome most of difficulties related to industrial use of biocatalysts, that are the high costs of producing enough stable and long lifetime enzymes, their high sensitivity to operating conditions and impurities, too high substrate specificity, and difficult process controllability due to their variable characteristics. In this context, model-based characterization of the enzymatic process is a valuable tool in further process design, development, and optimization steps.

The present study is focused on studying the kinetics of enzymatic transformation of β-D-glucose (DG) in 2-keto-D-glucose (kDG) in the presence of P_2O_x (oxygen 2-oxidoreductase, EC 1.1.3.10). Generally, P_2O_x catalyzes oxidation of mono- and disaccharides specifically at C-2 position leading to 2-ketosugars (even if few sugars and dicarbonyl sugars are oxidized at position C-3 to give the corresponding 3-keto and 2,3-diketo derivatives, respectively; [3]). This specific oxidation reaction has been intensively studied over decades, being of high interest for the industrial small/large-size production of rare sugars or sugar-derivates, such as: D-fructose (and then D-mannitol), 2-keto-D-gluconic acid (and then D-isoascorbic acid), 2-deoxy-3-keto-gluconic acid (and then 1-deoxy-D-xylulose, which is precursor of the vitamins thiamine and pyridoxol; [4]), D-sorbitol, diaminosorbitol, diaminomannitol [4], D-galactose oxidation to 2-keto-D-galactose (and then reduction at C-1 to yield D-tagatose, a low caloric sweetener; [4,5]), alternative sweeteners based on the disaccharides oxidation (allolactose, gentiobiose, melibiose, isomaltose; [6]), other synthetic carbohydrates (e.g. reaction of 2-keto-aldoses with alkali or their dehydration; production of dicarbonyl sugars, etc.; [3,4]). The selective reaction is also used to produce several fine chemicals and drugs/antibiotics [7].

A quite large number of P_2O_x substrates have been studied, including selective C-2 oxidation of several saccharides, P_2O_x displaying a varied activity (usually expressed relatively to the D-glucose substrate): α- and β-D(+)-glucose, 1-β-aurothioglucose, 3-deoxy-D-glucose, 6-deoxy-D-glucose,

* Corresponding author. Tel.: +40 744 830308.
E-mail address: gmaria99m@hotmail.com (G. Maria).

1381-1177/$ – see front matter © 2011 Elsevier B.V. All rights reserved.
doi:10.1016/j.molcatb.2011.10.007

Nomenclature

A_{240}	spectrometric absorbance at 240 nm (relative units)
c_j	species j concentration, mM
$D = d\ln(V)/dt$	reactor content dilution rate, s^{-1}
k_{cat}	turnover number of the enzyme, s^{-1}
k_c, k_d	rate constants, s^{-1} $(U\,mL^{-1})^{-1}$
$k_{axl}\,a$	overall gas-liquid mass transfer coefficient, s^{-1}
K_j	enzyme Michaelis-Menten constant (relatively to the substrate c_j), or inhibition constant, mM, $mM^{\alpha j}$
m	number of observed species
M_w	water molecular weight, $g\,mol^{-1}$
n	Yano-Koya exponent
N	number of experimental points (recording times)
p	number of model independent parameters
r_j	species j reaction rate, $mM\,s^{-1}$, $U\,mL^{-1}\,s^{-1}$
r	number of (measured) observations
s_y, s_y^2	model error standard deviation, or variance (in relative terms, Eq. (3))
t	time (s), or statistical Student test
v_m	reaction rate constant, s^{-1}
V	liquid volume, L
Y	stoichiometric coefficient

Greeks

α_j	rate constant (inhibition exponent)
ε_S	elasticity coefficient related to the substrate
ε_{240}	molar extinction coefficient (in spectroscopy), $mM^{-1}\,mm^{-1}$
λ	wavelength (nm), or eigenvalues of the inverse of the modified parameter covariance matrix [8,42]
μ_m	turnover number of the enzyme, $mM\,s^{-1}$ $(U\,mL^{-1})^{-1}$
ρ_w	water density, $g\,L^{-1}$
σ	measurement error standard deviation, mM, $U\,mL^{-1}$
π_{Km}	elasticity coefficient related to the Michaelis-Menten constant

Index

o	initial
ox	electron acceptor compound

Superscipts

*	saturation
$\hat{}$	estimated

Abbreviations

ABTS	2.2′-azinobis(3-ethylbenzthiazoline-6-sulfonic acid)
DG	D-Glucose
DO	dissolved oxygen
FAD	flavine-adenosine-dinucleotide
$FADH_2$	reduced form of FAD
GOD	glucose oxidase
kDG	2-keto-D-glucose
MMA	adaptive random search of Maria [40]
NAD(P)H	Nicotinamide adenine dinucleotide (phosphate)
P_2O_x	pyranose 2-oxidase
S	substrate
$\|\|\cdot\|\|_2$	Euclidean norm

1,5-anhydro-D-glucitol, L(−)-sorbose, D-gluconolactone, D(+)-xylose, D-allose, 5-thioglucose, D-gentiobiose, 2-deoxy-D-glucose, D-galactose, D-melibiose, maltose, mannose, sucrose, lactose, trehalose, D-arabinose, dextrin, starch, glycerol, etc. [4,8–12].

In nature, P_2O_x is widely distributed in fungi, being a constituent of the ligninolytic system supplying peroxidases with hydrogen peroxide, or being involved in a secondary metabolic pathway converting D-glucose to cortalcerone (a fungal pyrone-antibiotic; [4]). However, its metabolic role in fungi remains unclear, although there is evidence of its important role in lignin degradation [9]. Wild-type P_2O_x is obtained from *Peniophora gigantea* [3,8,10], *Phanerochaete gigantea* [3], *Phanerochaete chrysosporium* [9], *Polyporus obtusus, Trametes versicolor, Lenzites betulinus, Pleurotus ostreatus, Phlebiopsis gigantea* [9], *Coriolus hirsutus, Coriolus versicolor, Daedaleopsis styracina, Gloeophyllum sepiarium* [11], *Tricholoma matsutake* [12], *Trametes hirsuta, Trametes ochracea, Aspergillus nidulans, Lyophyllum shimeji* (review of Bastian et al. [3]), etc. To improve the stability and catalytic activity of P_2O_x, the enzyme was modified by cloning the encoding gene from a fungal source and expressing it in *Escherichia coli* [3,13].

P_2O_x is a large homotetrameric protein with a molecular mass depending on the enzyme source, ranging from 250 to 322 kDa, and includes four subunits of identical size, and four molecules of flavine-adenosine-dinucleotide (FAD) per tetramer [9,14–16]. The FAD cofactor is covalently linked to the protein and couples the oxidation of carbohydrates to the subsequent production of H_2O_2 [9].

There are also analytical applications of P_2O_x in clinical chemistry, microbial process monitoring, or production of biosensors or biofuel cells [3,5,9,15,17]. To increase the enzyme activity and substrate sensitivity in a β-D(+)-glucose biosensor, the recombinant enzyme should display smaller K_{DG} and higher k_{cat} values comparatively to the wild-type.

The approached reaction in the present study is of particular importance for the production of high purity fructose from D-glucose in two steps (Cetus process; [18,19]). On the first step, DG is oxidized to kDG using P_2O_x at 25–30 °C and pH = 6–7 with very high conversion and selectivity, leading to a product free of allergenic compounds traces (such as aldose). Then, the kDG is reduced to D-fructose by NAD(P)H-dependent aldose reductase at 25 °C and pH = 7, the $NAD(P)^+$ being (in situ or externally) regenerated and re-used [18,20,21]. The process drawbacks are related to the very fast deactivating of P_2O_x by H_2O_2, and by the costly regeneration of $NAD(P)^+$ (the chemical reduction of kDG to D-fructose is also possible on Pt/C or Pd/C catalysts with molecular hydrogen at high pressures; [19]). However, current efforts tend to overcome most of these difficulties by increasing the enzyme half-life with the addition of catalase, by modifying P_2O_x structure [3,13], or by co-immobilizing P_2O_x on a suitable support [16,19,22].

The fructose is currently produced on a large scale by enzymatic isomerisation of glucose over some salts at 50–60 °C and pH = 7–8.5 [23]. The process, intensively studied and kinetically characterized, suffers from a series of inconvenients: glucose conversion is limited to the equilibrium level of ca. 50%, making the subsequent fructose separation in large chromatographic columns be very costly; glucose isomerase presents a poor stability, making its purification and immobilization difficult; calcium ions (from preliminary starch saccharification) have to be removed prior to glucose isomerisation; fructose product is still impurified by several saccharide-derivates.

Enzyme characteristics (activity, stability, cost, availability) and the process kinetics are of a highly engineering interest for process further development. On one hand free-enzyme batch or semi-batch reactors can be preferred when enzymes exhibit a high deactivation rate, it is cheap and product can be easily separated.

On the other hand, the use of immobilized enzymes offers an easy product separation, less enzyme loss, increased enzyme stability, enzyme protection against harmful environmental stress, and a better control of the process. Enzyme immobilization is made on a porous or nonporous suitable support made from a large variety of materials tailored (by functionalization, cross-linking, copolymerisation, crystallization, covalent binding) to increase the enzyme stability with less affecting its activity. However, immobilization is costly and leads to a considerable activity decrease due to the matrix-enzyme interactions and due to resistance introduced by the diffusion transport through support. Moreover, when the enzyme deactivation rate is high enough (of high order), the use of fixed-bed/mechanically agitated reactors with immobilized enzymes might become too costly, requiring frequent biocatalyst regeneration or replacement [24,25].

The key-point in solving the engineering aspects (reactor constructive, operation, and control solution) is the thermal and chemical stability of the enzyme, expressed by its half-time under certain operating conditions [26]. Besides, the optimal design and operation solution of the enzymatic reactor (e.g. flexibility vs. raw-materials and enzyme variability) is related to the knowledge of an adequate and reliable process kinetics/enzyme inactivation model based on the process mechanism. Recently Maria & Cocuz [27] determined the optimal operating solutions for a batch/semi-batch reactor with suspended enzyme for the DG oxidation with P_2O_x using a reduced model from the literature.

The aim of this paper is to derive a comprehensible kinetic model for the DG oxidation in the presence of P_2O_x and catalase, based on a mechanism that accounts for interference between the main and side-reactions. Systematic isothermal experiments (30 °C and optimal pH = 6.5) lead to determine the kinetic curves of several involved species for various amounts of added catalase. Experiments have been conducted using free enzymes (commercial grade recombinant P_2O_x from Sigma–Aldrich, obtained by expressing its gene from *Coriolus sp.* in *E. coli*). The proposed model includes the main reaction (of Ping-Pong–Bi-Bi kinetic type), but also P_2O_x inactivation by the H_2O_2 produced, and in situ H_2O_2 decomposition by catalase (of a generalized Yano-Koya kinetics). P_2O_x activity studies from literature suggest no significant changes in the enzyme rate constants by its immobilization [22]. While the presence of catalase drastically slows down the P_2O_x inactivation, a considerable decrease of the main reaction rate is observed in the present study. The derived kinetic model can be used for further process design and reactor optimization, its parameters being easily adaptable for every type of P_2O_x used.

2. Kinetic properties of P_2O_x

The reaction catalyzed by P_2O_x is of Ping-Pong–Bi-Bi type, typically found in flavoprotein oxidoreductases, and consists of a reductive half-reaction, in which an aldopyranose substrate reduces the FAD cofactor to yield $FADH_2$ and 2-ketoaldose (oxidation of the sugar at position C-2), followed by an oxidative half-reaction of re-oxidation of $FADH_2$ by the electron acceptor. If dissolved oxygen (DO) is used, a C-4a-hydroperoxyflavin intermediate is formed during this oxidative half-reaction [5].

Oxidation of DG with P_2O_x occurs with various forms of electron acceptor: molecular oxygen, quinones (such as 1,4-benzoquinone or its derivates, 1,2-naphthoquinone, 1,2-naphthoquinone-4-sulfonic acid; [5,28]), complexed metal ions and radicals, such as ferricenium ion Fc^+ (ferricenium hexafluorophosphate), phenazine methosulphate, potassium ferricyanide, 2,6-dichloroindophenol, ferrocene-methanol, ferrocene-carboxylic acid, nitroxide radical, potassium ferricyanide, 2,6-dichloroindophenol, ABTS cation radical [5,28–30].

If "ox" denotes the electron acceptor compound used, the DG oxidation with P_2O_x obeys the Ping-Pong–Bi-Bi rate expression [28,30]:

$$r = \frac{v_m c_{DG} c_{ox}}{K_{DG} c_{ox} + K_{ox} c_{DG} + c_{DG} c_{ox}} \quad (1)$$

(where c_j = species j concentration). The intrinsic mechanism involves in fact, eight elementary steps, the corresponding rate constants being related to the apparent v_m, K_{DG}, and K_{ax} constants (see Wohlfahrt et al. [28] for a detailed discussion). Separate estimation of these intrinsic constants is laborious due to required steady experiments to determine the dynamics of reaction intermediates (i.e. oxidant complexes). The rate constants of expression (1), or the basic Michaelis constants of P_2O_x can be estimated from initial reaction rates or from Lineweaver–Burk/Eadie–Hofstee plots [31], being reviewed in Table 1 for various reaction conditions and enzyme sources.

P_2O_x inactivates quickly under the degradative action of H_2O_2, kDG, and other reactive oxygen species resulted during DG oxidation. To prevent that, the common alternative is to remove the resulted H_2O_2 by its decomposition in the presence of catalase added in various amounts (100-fold excess to 1000-fold excess vs. P_2O_x; [18,22]). The in situ oxygen produced from H_2O_2 decomposition is an important source of electron acceptor for the main reaction [16]. However, both P_2O_x and catalase present only a limited stability as homogenous catalysts under process conditions [19]. In addition to H_2O_2, the hydroxyl radical is produced in a Fenton-type reaction when Fe^{2+} is present in traces, playing an important role in the P_2O_x inactivation [8].

Co-immobilization of P_2O_x and catalase (in a 1/30–1/1000 U U^{-1} ratio) on glyoxal agarose beads leads to up to 10-time decrease of the P_2O_x specific consumption, while a first-order P_2O_x inactivation in respect to H_2O_2 is observed [16]. However, immobilization introduces a considerable resistance to the mass transfer, requiring a low P_2O_x density on the carrier [16]. Besides, it seems that immobilization does not significantly change the enzyme rate constants, even if its stability is improved very much (up to 9 days half-life; [22]). An alternative is to improve the stability of P_2O_x and catalase by chemical modification prior to immobilization. For instance, by cross-linking the enzymes with Diimido-Esters, the most accessible and active protein amino groups are blocked, being thus protected against the kDG product action, the resulting P_2O_x activity being ca. three-times higher than the native enzyme [19].

Complex enzymatic systems, such as P_2O_x/laccase/catalase and another oxidative agent (e.g. quinones) leads to a self-regeneration system of high specific productivity, even though oxygen is rate limiting, by keeping a low H_2O_2 concentration in the proximity of the enzymes, thus preventing their fast specific consumption [16].

Leitner et al. [18] studied the dependence of the obtained residual P_2O_x activity (from *Trametes multicolor*) on the added catalase amount, for 100 mM DG oxidation at 25 °C and pH = 6.5 for 24 h. They determine a sigmoidal curve shape of this dependence, by indicating a Catalase/P_2O_x ratio of 300 U U^{-1} to preserve 50% of P_2O_x initial activity, while ratios higher than 1000 U U^{-1} keep the same 70% residual activity. Freimund et al. [10] recommend a Catalase/P_2O_x initial ratio of 300 U U^{-1} to protect the P_2O_x activity, Machida & Nakanishi [11] a ratio of 160 U U^{-1}, while Huwig et al. [22] successfully used an initial Catalase/P_2O_x ratio of 100 U U^{-1}.

The optimal conditions for DG oxidation with P_2O_x depend on the enzyme source: 25–30 °C, pH = 6.5–7 [8,14]; 55 °C, pH = 8–8.5 [9]. The P_2O_x activity and stability are strongly dependent on temperature and pH. For instance, P_2O_x from *Phanerochaete chrysosporium* retains more than 85% of its activity at pH = 4–11 after 1 week of storage at 4 °C. Also, P_2O_x retains 100% of its activity at 60 °C, 65% at 70 °C, and 35% at 75 °C after 2 h in 50 mM Tris–HCl buffer of pH = 8 [9]. For P_2O_x obtained from *Coriolus versicolor* (wild

Table 1
Reported apparent rate constants (v_m, k_{cat}, K_{DG}, K_{ax}) for D-glucose oxidation with P_2O_x under various conditions. Notations: DG = D-glucose; "ox" = oxidant agent; "wild" = native wild-type P_2O_x; "recomb." = recombinant P_2O_x obtained by its gene expression in host cells; "immob." = immobilized enzyme; "free" = experiments using free P_2O_x; rate expressions: $r = v_m c_{DG}/(K_{DG} + c_{DG})$, or $r = v_m c_{DG} c_{ox}/(K_{DG} c_{ox} + K_{ox} c_{DG} + c_{DG} c_{ox})$; $v_m = k_{cat} c_{P_2O_x,o}$.

K_{DG} (mM)	K_{ax} (mM)	v_m (s^{-1})	k_{cat} (s^{-1})	Conditions	Enzyme source	Reference
63.5	0.26		0.089[a]	25 °C; pH = 6.5–7; $[DG]_o$ = 220 mM; $[P_2O_x]_o$ = 0.5 U mL^{-1}; k_{axI} a = 0.02 s^{-1}	*Peniphora gigantea*	[8] [e]
50	(DO) 0.48 (quinone) 6.9	503		35 °C; pH = 5.5; $[DG]_o$ = 100 mM; $[ox]_o$ = 2–5 mM	*Aspergillus niger*	[28]
(wild) 1.1 (recomb.) 0.4–0.8		10.4 2.7–22.5[b]		44 °C; pH = 4.5–6 22 °C; pH = 7; $[DG]_o$ = 0.28 mM (immobilized, [22])	*Peniphora gigantea* (wild; recomb. *E. coli*)	[3,14,22]
(free) 0.85 (immob.) 0.79	(DO) 0.11 (quinone) 0.3		(free) 49 (DO) 70 (quinone) 324	30 °C; pH = 5; $[DG]_o$ = 500 mM	horseradish (wild) *Trametes multicolor* (recomb. *E. coli*)	[16]
1.43	(DO) 0.083	26.64[c]	111	55 °C; pH = 8–8.5; $[DG]_o$ = 50 mM	*Phanerochaete chrysosporium*	[9]
(wild) 0.94 (recomb.) 0.44–3			(wild) 48 (recomb.) 0.2–88	30 °C; pH = 6.5; $[DG]_o$ = 100 mM; DO as oxidant	*Trametes multicolor* (wild; recomb. *E. coli*)	[5]
(wild) 18.66 (recomb.) 20.70		(wild) 7.94 (recomb.) 10.81[b]		20 °C; pH = 5.5; $[DG]_o$ = 330 mM	glucose oxidase (EC 1.1.3.4) from *Aspergillus niger* (wild; recombinant in *Saccharomyces cerevisiae*)	[17]
(wild) 1.4 (recomb.) 0.74			(wild) 59.9 (recomb.) 70.6	37 °C; pH = 7; $[DG]_o$ = 0.1 mM	*Coriolus versicolor* (wild; recomb. *E. coli*)	[15]
1.0		0.02[c]	106[d]	22 °C; pH = 7; $[DG]_o$ = 0.1 mM	*Coriolus versicolor* (wild; recomb. *E. coli*)	[15]
0.74			54		*Trametes multicolor*	[13,29]
1.1			56		*Peniophora gigantean*	
5.0			9.4		*Peniophora sp.*	
1.7					*Coriolus hirsutus*	[11]
0.9				25 °C; pH = 7.5; $[DG]_o$ = 0.8 mM	*Coriolus versicolor*	
1.0					*Daedaleopsis styracina*	
1.8					*Gloeophyllum sepiarium*	
1.2		8.2[b]	40.5	30 °C; pH = 6.5; $[DG]_o$ = 0.1 mM	*Phlebiopsis gigantea*	[41]
1.28		26.6[b]	111	37 °C; pH = 7; $[DG]_o$ = 0.0033 mM	*Tricholoma matsutake*	[12]

[a] Units in s^{-1} (U/mLs)$^{-1}$; 1 U of P_2O_x activity is defined as the amount of enzyme necessary for the oxidation of 1 μmol of ABTS per minute under the given conditions (ABTS = 2.2′-azinobis(3-ethylbenzthiazoline-6-sulfonic acid)(e.g. 30 °C and pH = 6.5, [14]).
[b] Units in μmol min^{-1} mg-protein^{-1}.
[c] Units in U mg-protein^{-1}.
[d] Units in s^{-1} g^{-1}.
[e] Rate expression is an approximation of the Ping-Pong–Bi-Bi reaction, i.e.: $r = v_m c_{DG} c_{ox}/(K_{DG} K_{ox} + K_{DG} c_{ox} + K_{ox} c_{DG} + c_{DG} c_{ox})$ (non-competitive inhibition with the substrate *DG* and "ox").

and recombinant in *E. coli*), the optimum reaction conditions are pH = 6–8 and 40–60 °C, the enzyme being stable for pH = 5–9 and for temperatures below to 65 °C [11,15]. For P_2O_x obtained from *Tricholoma matsutake*, the optimum reaction conditions are pH = 7–7.5 and 50–55 °C, the enzyme being stable for pH > 6 and for temperatures below to 55 °C [12]. For P_2O_x obtained from *Trametes multicolor*, the optimum reaction conditions are pH = 5.5–6.5 (DO as oxidant) and 55 °C [29]. The optimum pH is also dependent on the electron acceptor used, varying between 4 and 8 [29].

Recombinant P_2O_x's are molecularly designed to satisfy the application goal: for construction of an enzymatic biosensor for DG detection, low enzyme K_{DG} and high k_{cat} values are desirables comparatively to the wild-type [15,17]. The explanation can be given by the expression of the reaction rate relative sensitivity coefficients expressed vs. the substrate (the so-called ε-elasticity coefficient), or vs. the Michaelis–Menten constant (the so-called π-elasticity coefficient) [32]:

$$\varepsilon_S = \frac{\partial \ln(r)}{\partial \ln(S)} = \frac{K_m}{K_m + S}; \pi_{K_m} = \frac{\partial \ln(r)}{\partial \ln(K_m)} = -\varepsilon_S; \quad (2)$$

(where S = substrate; r = reaction rate; K_m = Michaelis–Menten constant). For an industrial use, a high sensitivity of reaction rate to substrate is not very crucial, but a low sensitivity to the rate constant is desirable to better control the process vs. its structural changes.

Various chemicals can inhibit the P_2O_x activity at various degrees, such as: $HgCl_2$, $(NH_4)_2SO_4$, $ZnCl_2$, $MnCl_2$, $NiCl_2$, $AgNO_3$, lead acetate, $CuCl_2$, $MnCl_2$ [9], CoSO4, CuSO4, ZnSO4, α,α′-dipyridyl, o-phenanthroline, 8-hydroxyquinoline, p-chloromercuribenzoate [11].

3. Experimental

3.1. Enzymes and reagents

The following substances were used for the present study: recombinant pyranose 2-oxidase (EC 1.1.3.10, product number P4234, activity of 10.4 U mg-protein^{-1}) from *Coriolus sp.* expressed in *E. Coli*; catalase (EC 1.11.16, product number C1345, activity of 2860 U mg-protein^{-1}) from bovine liver; glucose oxidase (GOD, EC 1.1.3.4, product number G2133, activity of 154 U mg-protein^{-1}) from *Aspergillus niger*; β-D-glucose; peroxidase (EC 1.11.1.7. product number P6782, activity of 1000 U mg-protein^{-1}) from horseradish; 2,2-azinobis(3-ethylbenz-thiazoline-6-sulfonic acid) (ABTS); 0.1 M acetate buffer solution of pH = 5.0; 0.05 M phosphate buffer solution of pH = 6.5; 0.01 M phosphate buffer solution of pH = 6.5. All chemicals were purchased from Sigma – Aldrich and used without further purification.

Glucose conversion assessment was achieved by using the method of De Luca et al. [33], relating changes in UV fluorescence emission spectra with the glucose concentration of samples in the presence of free GOD. The effect of glucose addition is an increase in the peak value and area of the fluorescence intensity emission spectrum, since reduced and oxidized flavins ($FADH_2$ and FAD)

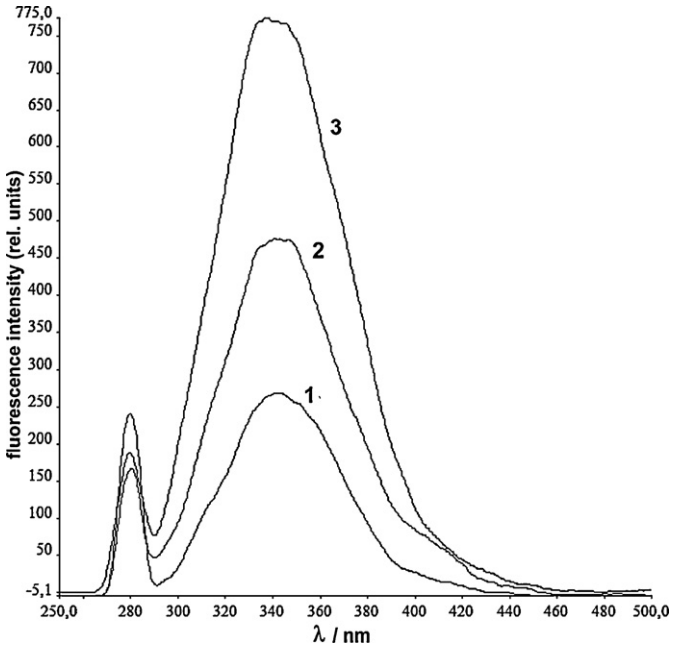

Fig. 1. Fluorescence emission spectra (λ-excitation = 278 nm; λ-emission = 340 nm): (1) without glucose; (2) with 1 mM glucose; (3) with 2 mM glucose.

exhibit different fluorescent properties. The approach exploits the UV intrinsic fluorescence of some amino acids from GOD, basically tyrosine and tryptophan. This fluorescence is characterized by an excitation with two maxima at 224 nm and 278 nm, and an emission around 340 nm, being usually employed to get information about enzyme configuration and bonding positions.

The D-glucose determination procedure is the following: in the spectrophotometer tank, 50 μl of reaction mixture sampled from bioreactor is diluted at 2.97 mL with 0.1 M acetate buffer solution of pH 5.0; the mixture is gently homogenised and incubated at 25 °C for 1 min. The emission fluorescence spectra have been collected by means of a spectrofluorimeter (model LS 50, Perkin–Elmer), by using as light source a Xenon discharge lamp with an emission spectrum ranging from 200 nm to 800 nm immediately after addition of 30 μl GOD (7 U mL^{-1}). Sample excitation was performed at 278 nm, while the emission spectrum was recorded in the range of 250–500 nm. The spectra have been acquired with an entrance slit fixed at 5 nm and an exit slit fixed at 8 nm with a scan speed of 100 nm s^{-1}. The emission fluorescence spectrum for the DG corresponds to the integral area in the region of 290–400 nm (see a typical emission fluorescence spectra of GOD in Fig. 1, in the presence or absence of glucose).

P_2O_x activity was monitored by observing the rate of oxygen consumption during the reaction (using an oxygen electrode, Rank Brothers Ltd.) in the thermostatically controlled laboratory bioreactor. Pyranose oxidase activity was determined spectrophotometrically at 420 nm, following the procedure of Leitner et al. [18], by measuring at 30 °C the formation of H_2O_2 in a peroxidase-coupled assay using ABTS (ε_{420} = 43,200 M^{-1} cm^{-1}) as the chromogen. The standard assay mixture (3 mL total) contained 3 μmol ABTS in potassium phosphate buffer (50 mM, pH 6.5), 2 U horseradish peroxidase, and 100 μL sample from bioreactor. One unit (U) of P20x activity is defined as the amount of enzyme necessary for the oxidation of 2 μmol of ABTS per minute under the given conditions. Enzyme assays were performed in triplicate and mean values are given. The procedure was repeated for every undertaken sample from the bioreactor during the reaction.

Catalase activity is expressed in Sigma units and was measured according to the instructions of the supplier (Sigma, [34]). One unit will decompose 1.0 μmol of H_2O_2 per minute at pH 7.0 and 25 °C.

Hydrogen peroxide concentrations were confirmed by UV absorption measurement at 240 nm. In the ultraviolet range, H_2O_2 displays a continuous increase in absorption with the decreasing wavelength. The decomposition of H_2O_2 by catalase can be followed directly by the decrease in absorbance at 240 nm (molar extinction coefficient of $\varepsilon_{240} = 0.00394 \pm 0.0002$ mM^{-1} mm^{-1}). The difference in absorbance (ΔA_{240}) per time unit is a measure of the catalase activity [35].

3.2. Batch experiments of DG oxidation

Experiments have been carried out in a 2 L laboratory bioreactor (Biostat A Plus, Sartorius; 1 L reaction liquid), with the operating parameters (temperature, pH, DO, liquid-level) recorded and controlled by means of an on-line computer [36]. The six-blade disk impeller and baffles ensures a satisfactory homogenisation of the bioreactor content, while the air micro-sparger system ensures a good gas-liquid contact, the bubble size being dependent on the aeration rate.

Separate experiments, under various operating conditions, allowed determining and correlating the overall gas–liquid mass transfer coefficient $k_{axl}\,a$ with the aeration and mixing rates (for the same liquid volume, temperature, sparger depth, and system geometry; [36]). A simple, non-invasive procedure has been applied, conducted in the absence of reaction, and involving repeated liquid de-aeration (even if not complete) by sparging with compressed N_2, followed by re-aeration. The dissolved oxygen kinetic curves recorded lead to evaluate the $k_{axl}\,a$ coefficient. Values of 0.005–0.01 s^{-1} (distilled water) and 0.01–0.02 s^{-1} (reaction medium) have been determined under optimal aeration conditions of 1 L min^{-1} rate and 300 rpm stirrer rotational speed.

For studying the DG enzymatic oxidation with P_2O_x, the experiments have been conducted in the optimal oxygenation conditions (using compressed air introduced through the ring sparger), in the absence of catalase, or using various amounts of catalase in the range of 0–80.4 U mL^{-1}. (i.e. 0–300 U U^{-1} Catalase/P_2O_x ratio). Experiments with higher Catalase/P_2O_x ratios are not interesting from the engineering point of view, as long as the main reaction rate decreases sharply with the catalase amount in the reaction environment. Free enzyme experiments have been conducted using 100 mM glucose, 0.25 U mL^{-1} P_2O_x, 10 mM phosphate buffer solution, pH = 6.5, and 30 °C. DO was recorded by means of the reactor pO_2 electrode, while small samples taken during reaction have been separately analyzed to determine the concentration of glucose (1 mL samples, aliquoted in vials and immediately stored up at −70 °C for future analyses), concentration of H_2O_2 (3 mL samples, immediately analyzed with the spectrophotometer), and the P_2O_x residual activity (100 μL samples, spectrophotometrically analyzed). The derived dynamic evolution of main species concentrations, displayed in the Figs. 3–5, is further used to estimate the kinetic model rate constants.

4. Modelling the oxidative process

The proposed kinetic model of the DG conversion to kDG is based on three main reactions (Fig. 2 and Table 2): D-glucose oxidation with dissolved oxygen in liquid (from sparging air) in the presence of P_2O_x; inactivation reaction of P_2O_x with the H_2O_2 produced during DG oxidation, with forming inactive species; decomposition of hydrogen peroxide in the presence of catalase and possible Fe traces (see Treitz et al. [8] and Maria [37] for the influence of

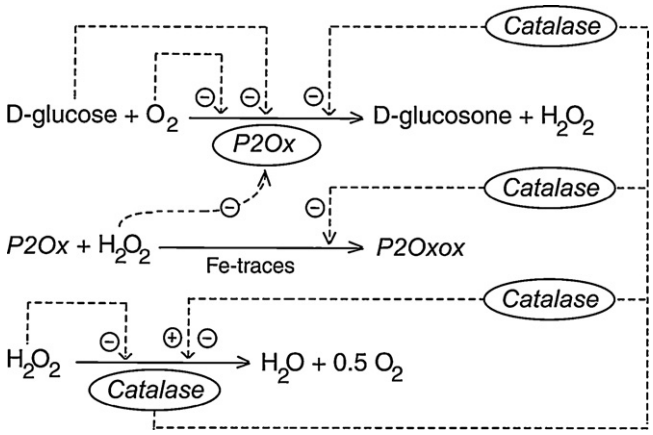

Fig. 2. The simplified reaction path for D-glucose enzymatic oxidation using P_2Ox and catalase. Perpendicular dash arrows on the reaction path indicate the catalytic activation, repressing or inhibition actions; absence of a substrate or product indicates an assumed concentration invariance of these species; ⊕/⊖ positive or negative action on the reaction rate.

larger amounts of Fe). Discussions on a possible mechanism for these reactions have already been presented in the literature [8,30].

Besides these information, there are several elements of novelty considered during elaboration of the proposed model, as follows (Table 2):

- the DG oxidation is considered, as in most of literature studies, being of Ping-Pong–Bi-Bi mechanism with the rate expression of Table 2; the reaction involves five reaction intermediates, but only three apparent rate constants (μ_m, K_{DG}, K_{DO}); the resulting D-glucosone (kDG) and H_2O_2 strongly influencing the P_2O_x activity;
- the hydrogen peroxide attack on P_2O_x is formally considered of second order, with a stoichiometric coefficient Y_{P2Ox} to be estimated together with the rate constants; the P_2O_x inactivation apparent reaction may involve several steps, difficult to be highlighted experimentally [8];
- the second order decomposition of H_2O_2 by the catalase is considered inhibited by the substrate, following a generalized uncompetitive inhibition of Yano-Koya type [38]; the reaction can also be initiated and maintained by ultraviolet light or Fe traces, occurring with formation of hydroxyl radicals by homolysis [8];
- the in situ resulted oxygen from the H_2O_2 decomposition participates in the DG oxidation;
- the dilution effect due to water resulted from H_2O_2 decomposition is considered in the reactor mass balance, even if its contribution to the total volume is very small (around 0.1%).

An ideal batch reactor model was adopted to simulate the process evolution under various initial conditions. Mass balance equations presented in Table 2 correspond to a perfectly mixed isothermal reactor, with explicitly accounting for the content dilution term [$D = d\ \ln(V)/dt$] due to water resulting from the H_2O_2 decomposition.

The rate constants of the model have been estimated based on three sets of recorded data including concentration profiles in time of DG, DO, H_2O_2, and P_2O_x in the absence of catalase, or with added catalase in an initial Catalase/P_2O_x ratio of 100 U U^{-1} or 300 U U^{-1}.

Table 2
Proposed kinetic model and batch operation for D-glucose oxidation using P_2O_x and of H_2O_2 decomposition using catalase (commercial recombinant P_2O_x from modified *E. coli* strain). Notations: DG = D-glucose; kDG = 2-keto-D-glucose; Catal. = catalase; D = average logarithmic volume growing rate; DO = dissolved oxygen; M_w = water molecular weight; ρ_w = water density; c^*_{DO} =saturation concentration of DO at the reaction temperature; $[H_2O]_r$ =water resulted from H_2O_2 decomposition.

Reactions:

$C_6H_{12}O_6 + Y_{ox}O_2 \xrightarrow[(water)]{P_2O_x} C_6H_{10}O_6 + H_2O_2$

$Y_{P_2O_x}P_2O_x + H_2O_2 \xrightarrow[(water)]{Fe\ traces} P_2O_x ox$ (Inactivated form)

$H_2O_2 \xrightarrow[(water)]{catalase} H_2O + 0.5O_2$

Rate expressions:

$r_{our} = \frac{\mu_m c_{P2O_X} c_{DG} c_{DO}}{(K_{DG} c_{DO} + K_{DO} c_{DG} + c_{DG} c_{DO})}$, (Ping-Pong-Bi-Bi mechanism; [28])

$r_d = k_d c_{P2O_X} c_{H_2O_2}$

$r_c = \frac{k_c c_{catal} c_{H_2O_2}}{\left(1 + K_{OH} c^n_{H_2O_2}\right)}$, (generalized uncompetitive inhibition Yano-Koya; [38])

Mass balance equations in batch operation mode:	Operating parameters: Content dilution:
$\frac{dc_{DO}}{dt} = k_{oxl} a(c^*_{DO} - c_{DO}) - Y_{ox} r_{our} + 0.5\, r_c - D\, c_{DO}$	
$\frac{dc_{DG}}{dt} = -r_{our} - D\, c_{DG}$	$D = \frac{1}{V}\frac{dV}{dt} = \frac{d[H_2O]_r}{dt}\frac{M_w}{\rho_w}$;
$\frac{dc_{kDG}}{dt} = r_{our} - D\, c_{kDG}$	$M_w = 18$ g mol^{-1}; $\rho_w = 996$ g L^{-1}
$\frac{dc_{POx}}{dt} = -Y_{POx} r_d - D\, c_{POx}$	$c^*_{DO} = 0.2484$ mM(fed air, 30°C)
$\frac{dc_{H_2O_2}}{dt} = r_{our} - r_d - r_c - D\, c_{H_2O_2}$	$k_{axl}\, a = 0.01$–0.02 s^{-1} [8,27]
$\frac{dV}{dt} = D\, V$	

A weighted least square criterion has been used as a suitable statistical estimator, due to different standard deviations of the observed species, the objective function minimizing the model error variance (in relative terms) [39]:

$$s_y^2 = \left(\frac{\left\|c_{DG} - \hat{c}_{DG}\right\|_2^2/\sigma_{DG}^2 + \left\|c_{DO} - \hat{c}_{DO}\right\|_2^2/\sigma_{DO}^2 + \left\|c_{H_2O_2} - \hat{c}_{H_2O_2}\right\|_2^2/\sigma_{H_2O_2}^2 + \left\|c_{P2Ox} - \hat{c}_{P2Ox}\right\|_2^2/\sigma_{P2Ox}^2}{(Nm - p)} \right), \quad (3)$$

(where N is the number of experimental points (recording times), m is the number of observed variables; p is the number of model independent parameters, $\hat{}$ denotes the model prediction values; $||\cdot||_2$ Euclidean norm of the residuals). The average experimental standard deviations are the following: $\sigma_{DG} = \sigma_{H_2O_2} = 1$ mM, $\sigma_{DO} = 0.1$ mM, and $\sigma_{P2Ox} = 0.05$ U mL^{-1}. An effective nonlinear programming solver, i.e. the adaptive random search MMA of Maria [40], has been used leading to the estimated parameters of Table 3.

The model predictions obtained are in a good agreement with the experimental data for all measured sets, as revealed by Figs. 3–5 for Catalase/P_2O_x ratios of 0–300 U U^{-1}. The model error, of ca. 2–3 mM for DG, is acceptable. The significance tests of the estimated rate constants are presented in Table 4 for the most relevant data set of Catalase/P_2O_x = 100 U U^{-1} characterized by larger number of data. By analysing the estimated rate constants of Tables 3 and 4, and the experimental results compared with the simulated species concentration dynamics (Figs. 3–5), several conclusions can be derived:

- the virtue of the proposed kinetic model is coming from its capacity to predict the process yield and enzyme inactivation degree using the Michaelis-type rate constants and Yano-Koya exponents independent of initial concentration of substrate or enzymes (P_2O_x and catalase);
- the estimated Michaelis constant of the P_2O_x (K_{DG}) and the k_{cat} are in the same range with the reported values in the literature for recombinant P_2O_x (Tables 1 and 4);
- almost all the parameters present high significance in the model according to the statistical tests of Table 4 (t-test

Table 3
Identified kinetic parameters for the D-glucose oxidation using P_2O_x and catalase (kinetic parameters for 30 °C, pH = 6.5; commercial recombinant P_2O_x from *Coriolus sp.*; $[DG]_0$ = 100 mM; $[P_2O_x]_o$ = 0.25 U mL^{-1}). Notations: DG = D-glucose; DO = dissolved oxygen.

Parameter	No catalase	Catal/P_2O_x = 100	Catal/P_2O_x = 300	Proposed correlations
μ_m, [mM s^{-1} (U mL^{-1}) $^{-1}$]	0.98778	0.36966	0.04970	$\mu_m = \mu_{mo}/\left(1 + K_m c_{catal}^{\alpha_m}\right)$ μ_{mo} = 9.8778 × 10^{-1}, mM s^{-1} (U mL^{-1})$^{-1}$ K_m = 2.0973 × 10^{-3}, mMα_m α_m = 2.0756
K_{DG}, (mM)		0.51905		
K_{DO} (mM)		14.545		
k_d, [s^{-1} (U mL^{-1}) $^{-1}$]	1.4204 × 10^{-3}	6.0781 × 10^{-4}	1.1528 × 10^{-4}	$k_d = k_{do}/\left(1 + K_d c_{catal}^{\alpha_d}\right)$ k_{do} = 1.4204·10^{-3}, s^{-1} (U mL^{-1})$^{-1}$ K_d = 3.7033·10^{-3}, mMα_d α_d = 1.8295
k_c, [s^{-1} (U mL^{-1}) $^{-1}$]	8.3 × 10^{-5} [a]	5.5560 × 10^{-5}	1.04 × 10^{-7}	$k_c = k_{co}/\left(1 + K_c c_{catal}^{\alpha_c}\right)$ k_{co} = 8.3000·10^{-5}, s^{-1} (U mL^{-1})$^{-1}$ K_c = 7.0944·10^{-10}, mMα_c α_c = 6.3255
K_{OH}, (mM^{-n})		0.58		
n		2.5765		
YP_2O_x, (U mL^{-1} mM^{-1})		0.01019		
k_{axl} a, (s^{-1})	0.02 [b]	0.01	0.01	[36]
s_y [c], (–)	1.76	2.01	2.22	

[a] Obtained by extrapolation.
[b] Approximated from separate in vitro tests.
[c] The model error standard deviation in relative values was computed using the formula (3).

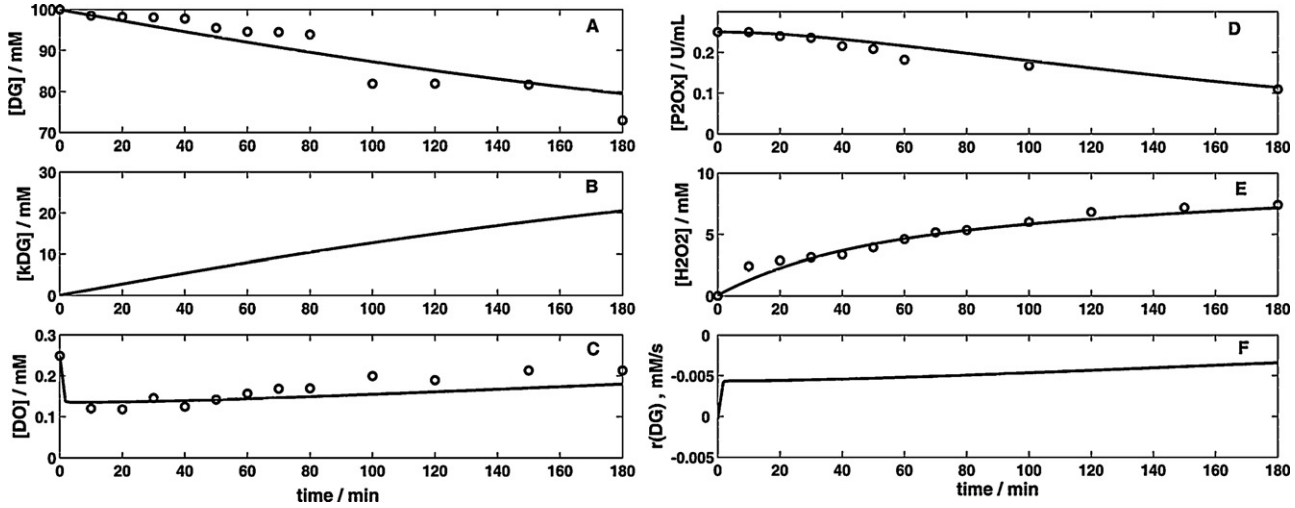

Fig. 3. Dynamics of species concentration (A–E) and DG-reaction rate (F) for D-glucose oxidation with air and pyranose 2-oxidase in the absence of catalase. Conditions: 100 mM glucose, 0.25 U mL^{-1} P_2O_x, 10 mM phosphate buffer, pH = 6.5; 30 °C. Model predictions are with a continuous line, and experimental values with points.

Table 4
Estimate significance tests for the D-glucose oxidation, for a catalase/P_2O_x = 100 ratio (t-tests calculated with the minimum noise standard deviation of $\tilde{\sigma} = 0.1$ (mM, or U mL^{-1}); see the Appendix of Treitz et al. [8] for details).

Parameter	Estimate	t-test[a]	ordered $\lambda_j/\tilde{\sigma}^{2}$ [b]	Intercorrelation matrix[c]								Reported value (Table 1)
K_{DO}, (mM)	14.545	22.2	1.0	1								0.11–0.48
K_{DG}, (mM)	0.519	0.004	3.2	0.10	1							0.4–5.0
μ_m, [mM s^{-1} (U mL^{-1})$^{-1}$]	0.369 (9.25 s^{-1})	19.4	8.1 × 10^{2}	0.95	0.40	1						– (0.2–88)
k_d, [s^{-1} (U mL^{-1})$^{-1}$]	6.078 × 10^{-4}	28.8	1.5 × 10^{4}	0.26	0.25	0.34	1					–
Y_{P2Ox}, (U mL^{-1} mM^{-1})	0.010	23.4	2.4 × 10^{6}	−0.07	−0.65	−0.28	−0.84	1				–
k_c, [s^{-1} (U mL^{-1}) $^{-1}$]	5.556 × 10^{-5}	25.3	4.5 × 10^{7}	−0.97	0.05	−0.88	−0.21	−0.03	1			–
K_{OH}, (mM^{-n})	0.58	11.1	1.0 × 10^{12}	−0.97	0.04	−0.88	−0.17	−0.07	0.99	1		–
n	2.576	42.0	3.1 × 10^{16}	0.80	0.27	0.83	0.76	−0.53	−0.74	−0.73	1	–

[a] The parameter is significant for t − test > t(Nm − p; 0.975) = 1.96.
[b] The ridge selection test of Maria & Rippin [42] is passed when $\lambda_j/\tilde{\sigma}^2 > 1$ [8,39].
[c] Absolute coefficients higher than 0.95 indicates highly intercorrelated parameters [8,39].

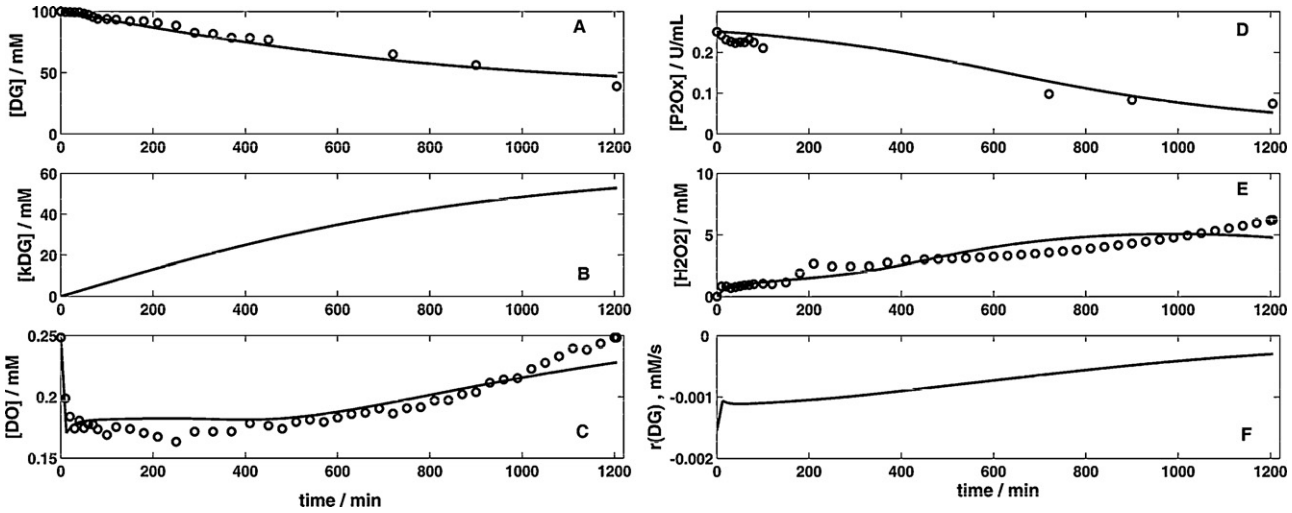

Fig. 4. Dynamics of species concentration (A-E) and DG-reaction rate (F) for D-glucose oxidation with air and pyranose 2-oxidase in the presence of 25 U mL^{-1} catalase (Catalase/P_2O_x = 100/1 U U^{-1}). Conditions: 100 mM glucose, 0.25 U mL^{-1} P_2O_x, 10 mM phosphate buffer, pH = 6.5; 30 °C. Model predictions are with a continuous line, and experimental values with points.

and $\lambda_j/\tilde{\sigma}^2$ test values higher than the relevant quantile 1.96 and the threshold 1, respectively); the confidence intervals have not been displayed being given by a linearized model formula [39];

- the Michelis-Menten type constants (μ_m, K_{DG}, K_{DO}) and those of the Yano-Koya inhibition model are well-known as being highly intercorrelated due to the hyperbolic model equation form. Absolute inter-correlations among them are sometimes more than 0.95, and laborious experiments are necessary to separate their influence on the reaction rate [39]. In the present case, the tests indicate K_{DG} as being difficult to be estimated as long as the glucose concentration is always much higher than the estimated K_{DG} value. Thus, K_{DG} was fixed to 0.52 mM, which is very close to the reported data in the literature (avg. 1.1 mM). Also the estimated K_{DO}, of higher values than those from literature, indicates the low influence of the [DG] on the main reaction rate on this studied concentration interval.
- the predicted P_2O_x residual activity by the model at longer run times (24 h) is in a good agreement with the reported data of Leitner et al. [18] at 25 °C, that is a 80% loss of activity for an initial Catalase/P_2O_x = 100 U U^{-1}, and a 50% loss of activity for an initial Catalase/P_2O_x = 300 U U^{-1} (plots not presented here).
- the stoichiometric coefficient Y_{P2Ox} of the H_2O_2 attack on P_2O_x is unchanged, irrespectively to the data set and catalase amount, indicating approximately 10 U P_2O_x inactivated by 1 millimole of H_2O_2 present in the liquid, that is a quite high inactivation capacity of hydrogen peroxide oxidant;
- the exponent $n \approx 2.6$ in the Yano-Koya rate expression of hydrogen peroxide decomposition indicates a high order reaction inhibition by large amounts of H_2O_2;
- the turnover numbers in all reactions (μ_m for DG oxidation, k_d for P_2O_x inactivation, k_c for H_2O_2 decomposition) are strongly influenced by the catalase concentration, roughly decreasing with one order of magnitude for Catalase/P_2O_x ratios increasing from 0 to 100 and then to 300 U U^{-1}. Consequently, a higher order of inhibition with catalase of these reactions is proposed, of generalized Yano-Koya type, by estimating the inhibition constant K_j ($j = m,d,c$) and exponent α_j. The results indicate a high order inhibition of the main reaction rate ($\alpha_m = 2.1$), and also for P_2O_x inactivation ($\alpha_d = 1.8$), and for H_2O_2 decomposition reaction ($\alpha_d = 6.3$);
- a direct consequence of such a high influence of catalase on the reaction rates is a considerable decrease of the P_2O_x inactivation with the Catalase/P_2O_x ratio, as reported in many

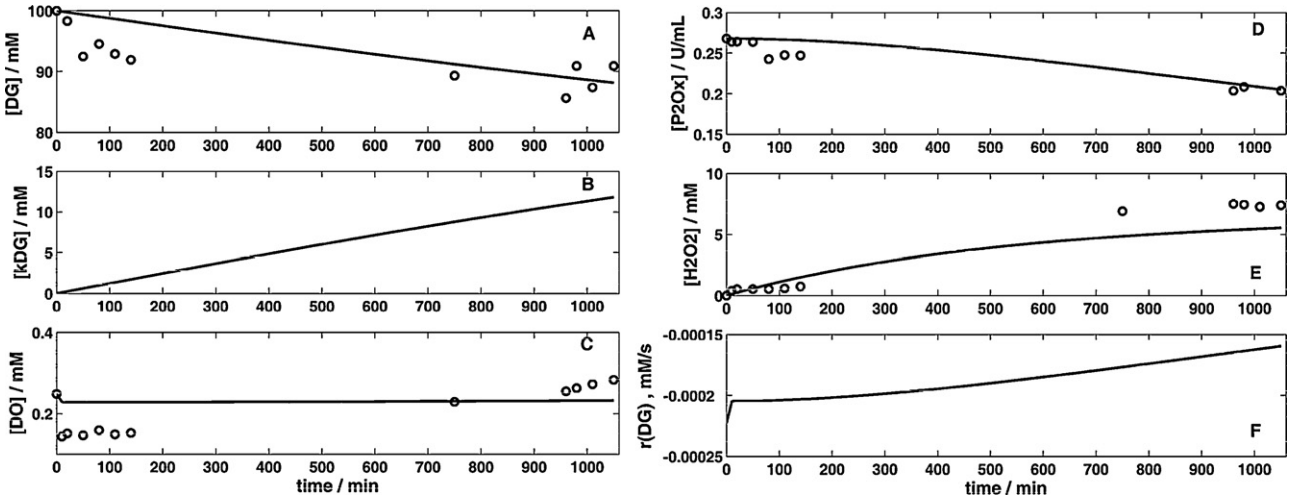

Fig. 5. Dynamics of species concentration (A–E) and DG-reaction rate (F) for D-glucose oxidation with air and pyranose 2-oxidase in the presence of 80.4 U mL^{-1} catalase (Catalase/P_2O_x = 300/1 U U^{-1}). Conditions: 100 mM glucose, 0.268 U mL^{-1} P_2O_x, 10 mM phosphate buffer, pH = 6.5; 30 °C. Model predictions are with a continuous line, and experimental values with points.

studies from literature. Simulations with the kinetic model indicate a 55% P_2O_x inactivation after 180 min of run without catalase, but the same inactivation is get after 790 min of run with a Catalase/P_2O_x = 100 U U^{-1} ratio, and after 7111 min of run with an initial Catalase/P_2O_x = 300 U U^{-1} ratio;

- unfortunately this favourable effect of catalase addition on the P_2O_x activity is counter-balanced by the drastic diminishment of the main reaction rate (i.e. the turnover number decrease). Simulations with the kinetic model reveal that a 20% DG conversion is obtained after 180 min of run without catalase, but the same conversion is obtained after 316 min of run with Catalase/P_2O_x = 100 U U^{-1} ratio, and after 2101 min with Catalase/P_2O_x = 300 U U^{-1} ratio. Analogously, 60% DG conversion is obtained after 1777 min of run with Catalase/P_2O_x = 100 U U^{-1} ratio, but no more than 33% conversion is obtained with Catalase/P_2O_x = 300 U U^{-1} ratio (if no additional P_2O_x is added during reaction).

In fact, as proved by Maria [26,37], for an enzymatic reactor with suspended enzyme of high order deactivation rate (more than one), the enzyme consumption for an imposed productivity can be drastically diminished (sometimes more than ten times) if an optimal enzyme feeding policy is adopted in a semi-batch or a pulse-like addition operation mode. In this context, the derived model in the present study can be used to perform engineering calculations for process design and optimization, by choosing an appropriate optimization function. Reactor optimization has to account not only for productivity vs. raw-materials (especially enzyme) and operational costs, but also for the P_2O_x enzyme inactivation characteristics, the effect of the added co-enzyme on the main reaction rate, optimal operation solution implementation, and process control costs. From such a perspective, a sufficiently adequate and reliable dynamic model of the process can lead to economic benefits at the expense of some computational steps to up-date its parameter when structural changes occur in the system (enzyme, raw-materials). The developed kinetic model, of fair quality and with enzyme parameters independent on the initial concentrations of species, fully justify such computational steps by accounting for antagonistic factors with influence on the enzymatic process.

5. Conclusions

Derivation of an enough adequate and reliable kinetic model for a complex multi-enzymatic process is a difficult task, requiring steady experimental efforts to get enough information on the process dynamics and its mechanism, and also extensive computational efforts to derive a comprehensible model with interpretable parameters. Such a model can be immediately valorised, as long as simple separate observations cannot give the whole picture on the process characteristics and interferences of the enzymatic reactions to be further used in engineering calculations.

The derived kinetic model for the D-glucose oxidation in the presence of P_2O_x and catalase reveals some interesting conclusions. The presence of catalase decreases very much the P_2O_x inactivation, from 4.4 times for a Catalase/P_2O_x = 100 U U^{-1} initial ratio vs. no-catalase-runs, to 39.5 times for a Catalase/P_2O_x = 300 U U^{-1} ratio. At the same time, the oxidation reaction rate is drastically diminished by the presence of catalase, from 1.8-times for a Catalase/P_2O_x = 100 U U^{-1} ratio, until 11.7-times for a Catalase/P_2O_x = 300 U U^{-1} ratio. Additionally, the running time necessary to get the same imposed conversion increases with the same ratio as the reaction rate diminishment.

The kinetic model is of satisfactory quality and robust, with enzyme parameters not depending on the initial concentration of species but only on the reaction conditions (temperature, pH). Model parameters are fully interpretable and of comparable values with the reported ones for similar reaction systems, offering the possibility to predict the process dynamics under various operating conditions. It is also to remark that in multi-enzyme reaction systems separate evaluations of enzyme characteristics and activity is not enough to derive pertinent conclusions as long as interferences among reactions occur. The kinetic model can be useful for an immobilized enzyme process alternative, offering predictions on the process dynamics if additional terms are added in the heterogeneous reactor mass balance equations [26]. As reported in the literature for the DG oxidation case, the estimated free P_2O_x rate constants do not suffer significant changes by enzyme immobilization. However, small adjustments will be necessary for secondary reactions rate constants.

The model applications are immediate. Thus, simulations of the batch or semi-batch process operation allow predicting the DG conversion for various amounts of P_2O_x and catalase initially added, or added during the reaction following a certain policy to be determined. The complex effects of the added catalase (P_2O_x life prolongation, and decline of the main reaction rate) imperatively require computational steps to determine the optimal amount of enzymes in respect to a specified economic objective (imposed conversion, or reactor productivity). Derivation of the optimal operation mode (batch, semi-batch, pulse) and optimal feeding policy (e.g. continuous or intermittent enzyme addition, following an uniform, exponentially like, or another addition policy [26,37]) can lead to a considerable save of enzyme. The kinetic model is also useful for further process design with parameters easily adaptable for every type of used P_2O_x.

Acknowledgments

Authors are grateful for the experimental facilities offered with generosity by Dr. Anicuta Stoica-Guzun and Dr. Marta Stroescu from the Laboratory of Mass Transfer of University Politehnica of Bucharest (Department of Chemical & Biochemical Engineering).

References

[1] P. Wang, Appl. Biochem. Biotechnol. 152 (2009) 343–352.
[2] M. Gavrilescu, Y. Chisti, Biotechnol. Adv. 23 (2005) 471–499.
[3] S. Bastian, M.J. Rekowski, K. Witte, D.M. Heckmann-Pohl, F. Giffhorn, Appl. Microbiol. Biotechnol. 67 (2005) 654–663.
[4] F. Giffhorn, Appl. Microbiol. Biotechnol. 54 (2000) 727–740.
[5] O. Spadiut, I. Pisanelli, T. Maischberger, C. Peterbauer, L. Gorton, P. Chaiyen, D. Haltrich, J. Biotechnol. 139 (2009) 250–257.
[6] C. Leitner, P. Mayr, S. Riva, J. Volc, K.D. Kulbe, B. Nidetzky, D. Haltrich, J. Mol. Catal. B: Enzym. 11 (2001) 407–414.
[7] G.S. Nyanhongo, G. Gübitz, P. Sukyai, C. Leitner, D. Haltrich, R. Ludwig, Food Technol. Biotechnol. 45 (2007) 250–268.
[8] G. Treitz, G. Maria, F. Giffhorn, E. Heinzle, J. Biotechnol. 85 (2001) 271–287.
[9] M.J. Artolozaga, E. Kubatova, J. Volc, H.M. Kalisz, Appl. Microbiol. Biotechnol. 47 (1997) 508–514.
[10] S. Freimund, A. Huwig, F. Giffhorn, S. Köpper, Chem. Eur. J. 4 (1998) 2442–2455.
[11] Y. Machida, T. Nakanishi, Agric. Biol. Chem. 48 (1984) 2463–2470.
[12] Y. Takakura, S. Kuwata, Biosci. Biotechnol. Biochem. 67 (2003) 2598–2607.
[13] M. Bannwarth, D. Heckmann-Pohl, S. Bastian, F. Giffhorn, G.E. Schulz, Biochemistry 45 (2006) 6587–6595.
[14] H.J. Danneel, E. Rössner, A. Zeeck, F. Giffhorn, Eur. J. Biochem. 21 (1993) 795–802.
[15] I.M. Nishimura, T. Minamihara, Y. Koyama, Biotechnol. Lett. 21 (1999) 203–207.
[16] P. Sukyai, T. Rezic, C. Lorenz, K. Mueangtoom, W. Lorenz, D. Haltrich, R. Ludwig, J. Biotechnol. 135 (2008) 281–290.
[17] Z. Zhu, C. Momeu, M. Zakhartsev, U. Schwaneberg, Biosens. Bioelectron. 21 (2006) 2046–2051.
[18] C. Leitner, W. Neuhauser, J. Volc, K.D. Kulbe, B. Nidetzky, D. Haltrich, Biocatal. Biotransform. 16 (1998) 365–382.
[19] Z. Shaked, S. Wolfe, Methods Enzymol. 137 (1988) 599–615.
[20] H.K. Chenault, G.M. Whitesides, Appl. Biochem. Biotechnol. 14 (1987) 147–197.
[21] M. Slatner, G. Nagl, D. Haltrich, K.D. Kulbe, B. Nidetzky, Biocatal. Biotransform. 16 (1998) 351–363.
[22] A. Huwig, H.J. Danneel, F. Giffhorn, J. Biotechnol. 32 (1994) 309–315.

[23] A. Liese, K. Seelbach, C. Wandrey (Eds.), Industrial Biotransformations, Wiley-VCH, Weinheim, 2006, p. 18.
[24] A. Moser, Bioprocess Technology: Kinetics and Reactors, Springer-Verlag, New York, 1988.
[25] A.J.J. Straathof, P. Adlercreutz, Applied Biocatalysis, Harwood Academic Publ., Amsterdam, 2005.
[26] G. Maria, Comput. Chem. Eng. 35, in press doi:10.1016/j.compchemeng.2011.06.006.
[27] G. Maria, A. Cocuz, Rev. Chim. 62 (2011) 318–327.
[28] G. Wohlfahrt, S. Trivic, J. Zeremski, D. Pericin, V. Leskovac, Mol. Cell. Biochem. 260 (2004) 69–83.
[29] C. Leitner, J. Volc, D. Haltrich, Appl. Environ. Microbiol. 67 (2001) 3636–3644.
[30] V. Leskovac, S. Trivic, G. Wohlfahrt, J. Kandrac, D. Pericin, Int. J. Biochem. Cell Biol. 37 (2005) 731–750.
[31] H.W. Blanch, D.S. Clark, Biochemical Engineering, Marcel Dekker, New York, 1997.
[32] R. Heinrich, S. Schuster, The Regulation of Cellular Systems, Chapman & Hall, New York, 1996.
[33] P. De Luca, M. Lepore, M. Portaccio, R. Esposito, S. Rossi, U. Bencivenga, D.G. Mita, Sensors 7 (2007) 2612–2625.
[34] Sigma Chemical Co., Sigma Manual, Sigma Chemical Co., St. Louis (MO), 1997.
[35] H.U. Bergmeyer (Ed.), Methods of Enzymatic Analysis, Enzymes 1: Oxidoreductases, Transferases, vol. 3, 3rd ed., Verlag Chemie, Weinheim, 1983.
[36] M.D. Ene, I. Jipa, G. Maria, A. Stoica-Guzun, M. Stroescu, Rev. Chim. 62 (2011) 227–232.
[37] G. Maria, Comput. Chem. Eng. 31 (2007) 1231–1241.
[38] K. Schügerl, K.H. Bellgardt (Eds.), Bioreaction engineering – Modelling and Control, Springer Verlag, Berlin, 2000, p. 60.
[39] G. Maria, Chem. Biochem. Eng. Q. 18 (2004) 195–222.
[40] G. Maria, ARS combination with an evolutionary algorithm for solving MINLP optimization problems, in: M.H. Hamza (Ed.), Modelling, Identification and Control, IASTED/ACTA Press, Canada, 2003, pp. 112–118.
[41] A. Schäfer, S. Bieg, A. Huwig, G.W. Kohring, F. Giffhorn, Appl. Environ. Microbiol. 62 (1996) 2586–2592.
[42] G. Maria, D.W.T. Rippin, Chem. Eng. Sci. 48 (1993) 3855–3864.